

Measurement of mass-energy distributions of fission fragments using time-of-flight method

V.I. Zagrebaev, E.M. Kozulin, K.V. Novikov

1. Fission of atomic nuclei

1.1 Fission barrier

The process of fission of the atomic nucleus when bombarded by slow neutrons was discovered in 1938 by Otto Hahn and Fritz Strassmann (the article was published in 1939). The term “fission” to refer to this unusual process was proposed by Otto Frisch and Lisa Meitner by analogy with the biological process of cell fission. In 1939 Niels Bohr and John Wheeler explained the mechanism of fission on the basis of the liquid-drop model of the atomic nucleus which they proposed and which has retained its relevance until today. An even more interesting phenomenon, non-induced (spontaneous) fission was discovered in 1940 by G.N. Flerov and K.A. Petrzhak.

In the liquid-drop model of the nucleus its mass (the sum of the masses of nucleons minus the binding energy) is given by the Weizsäcker formula which can be simplified in the following form

$$M(Z, A; \delta)c^2 = Zm_p c^2 + Nm_n c^2 - [a_v A - a_s S(\delta) - Z^2 f(\delta)]. \quad (1)$$

The first term in the square brackets reflects the total binding energy of all nucleons ($A = Z + N$) with their neighbors. Due to the short range of nuclear forces each nucleon interacts only with its immediate neighbors. The second term just takes into account the fact that the surface nucleons (their number is proportional to the surface area of the nucleus S) have fewer neighbors and are, therefore, less bound i.e. it is necessary to slightly reduce the total binding energy (hence, the minus sign). The last term takes into account the Coulomb repulsion of protons which also reduces the binding energy. The deformation of the nucleus increases its surface area, thus increasing the number of less bound surface nucleons, and the total binding energy decreases (the mass increases). In formula (1) the parameter δ is intended to describe the change of deformation: if $\delta = 0$ the nucleus has the spherical shape with the minimum surface for the given volume $S(0) = 4\pi R^2$. The Coulomb energy (proportional to the product of charges and inversely proportional to the distance between them) decreases with increasing deformation as in this case the average distance between the protons increases. This is taken into account by the factor $f(\delta)$ in the last term of the formula (1) which decreases with increasing δ .

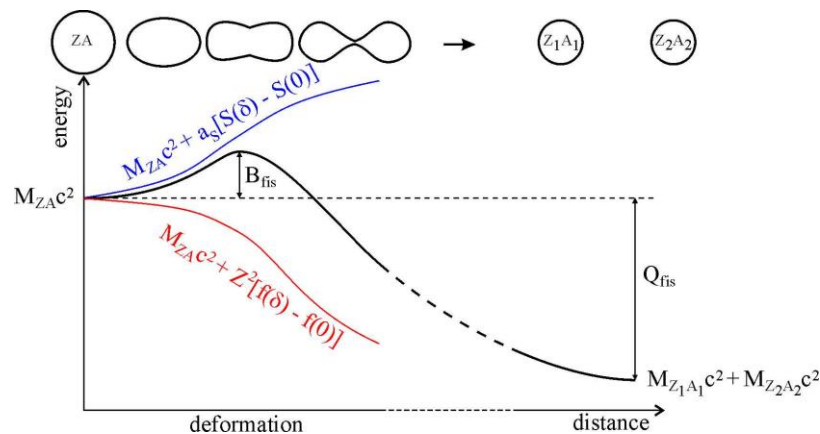


Fig. 1.1 Change of the energy of the nucleus with its deformation and subsequent fission.

Fig. 1.1 schematically shows change of the total energy of the nucleus $M(Z, A; \delta)c^2$ as well as its surface and Coulomb energies with increasing deformation. It also schematically shows the change in shape of the nucleus (Z, A) in the process of its fission into two fragments (Z_1, A_1) and (Z_2, A_2) . When these fragments go to the infinite distance, then by the law of energy conservation $M(ZA)c^2 = M(Z_1A_1)c^2 + M(Z_2A_2)c^2 + Q_{fis}$. Q_{fis} is the energy released in fission and revealing itself in the form of the kinetic energy of nuclear fragments and their excitation energy (subsequently removed by evaporation of neutrons and gamma-ray emission). For all heavy nuclei $Q_{fis} > 0$ and thus, it is energetically favorable to split into two more strongly bound fragments. However, this requires the nucleus to overcome the so-called fission barrier B_{fis} (see Fig. 1.1). The value of this barrier is very high for the nuclei with masses $A \sim 200$ and these nuclei are stable with respect to fission (they can undergo fission if their excitation energy exceeds the fission barrier). For heavier nuclei with $A \sim 240$ the fission barrier height is about 6 MeV and they already can undergo spontaneous fission.

Finally, note that the shape of the nucleus during fission is rather complicated and cannot be described using a single parameter. Fission occurs in the multidimensional space of deformation parameters and is regulated by the multidimensional energy surface with multiple local minima and saddle points due to the quantum (shell) properties of the nuclear system. All this, however, does not change the qualitative interpretation of the fission mechanism shown in Fig. 1.1.

The liquid-drop model of the nucleus [1] predicts a monotonic decrease of the fission barrier height with increasing charge of the atomic nucleus due to the increasing Coulomb energy. However, taking into account shell effects (arising from the quantum nature of the motion of nucleons in the mean field of the nucleus) leads to a significant change in this monotonous dependence and, in particular, a sharp increase in the height of the fission barrier for nuclei with closed shells [2]. Fig. 1.2 shows the theoretical estimations of the height of the fission barriers, made with and without shell corrections to the energy of the ground state of nuclei close to the line of stability. For some nuclei the experimental values of B_{fis} are also shown.

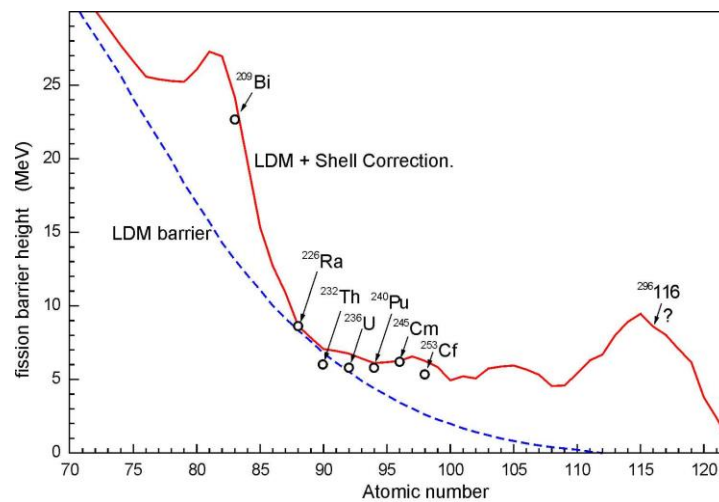


Fig. 1.2 Fission barriers of isotopes of heavy nuclei along the stability line. The dashed curve shows the calculation within the liquid-drop model of the nucleus [1]; the solid curve takes into account shell corrections [3]. For some nuclei experimental values of the height of the fission barriers are shown [4].

1.2 Lifetimes of spontaneously fissioning nuclei

With increasing charge of atomic nuclei their fission barriers are becoming lower and spontaneous fission starts to significantly affect their lifetimes. If the nucleus can undergo multiple modes of decay (alpha decay, beta decay, fission), then we should talk about the partial half-lives $T_{1/2}^\alpha$, $T_{1/2}^\beta$ and $T_{1/2}^{sf}$ which are inversely proportional to the corresponding decay probabilities for these channels (*sf* here means spontaneous fission). The experimental measurement of $T_{1/2}^{sf}$ is a very challenging task for both long-lived and short-lived nuclei. Besides, the value of $T_{1/2}^{sf}$ varies in a very wide range: from 10^{17} years to milliseconds. Fig. 1.3 shows the experimental spontaneous fission lifetimes for some even-even isotopes of several elements (as a rule, the probability of spontaneous fission of even-odd isotopes is much smaller). The theoretical estimation of the spontaneous fission lifetime may be made using empirical formulas on the website [5].

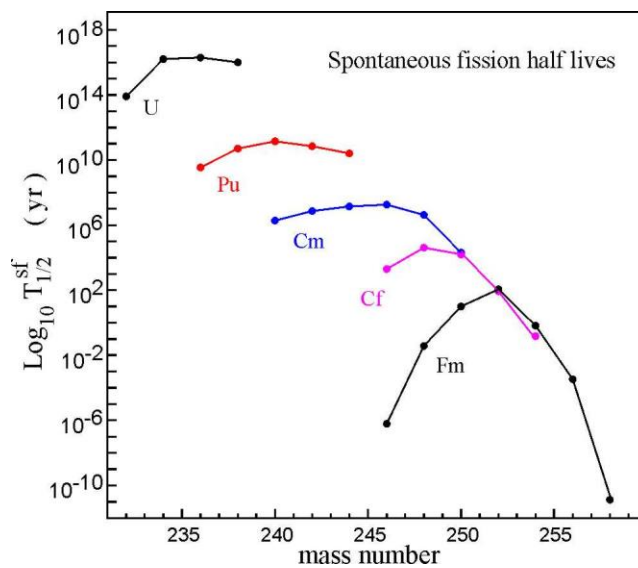


Fig. 1.3 Spontaneous fission half-lives of some even-even isotopes of uranium, plutonium, curium, californium and fermium [4].

1.3 Mass distribution of fission fragments

In the liquid drop model fission of the nucleus must always be symmetric i.e. fission fragments must have the same mass and charge. Indeed, for some heavy nuclei and in the fission of highly excited nuclei a symmetric mass distribution of fragments is observed. However, for most weakly excited nuclei mass distribution of fragments is strongly asymmetric. A classical example is fission of uranium nuclei by the capture of thermal neutrons (their excitation energy does not exceed 7 MeV). Fig. 1.4 shows the relative mass distribution of fission fragments of ^{236}U nuclei formed by the capture of thermal neutrons by ^{235}U .

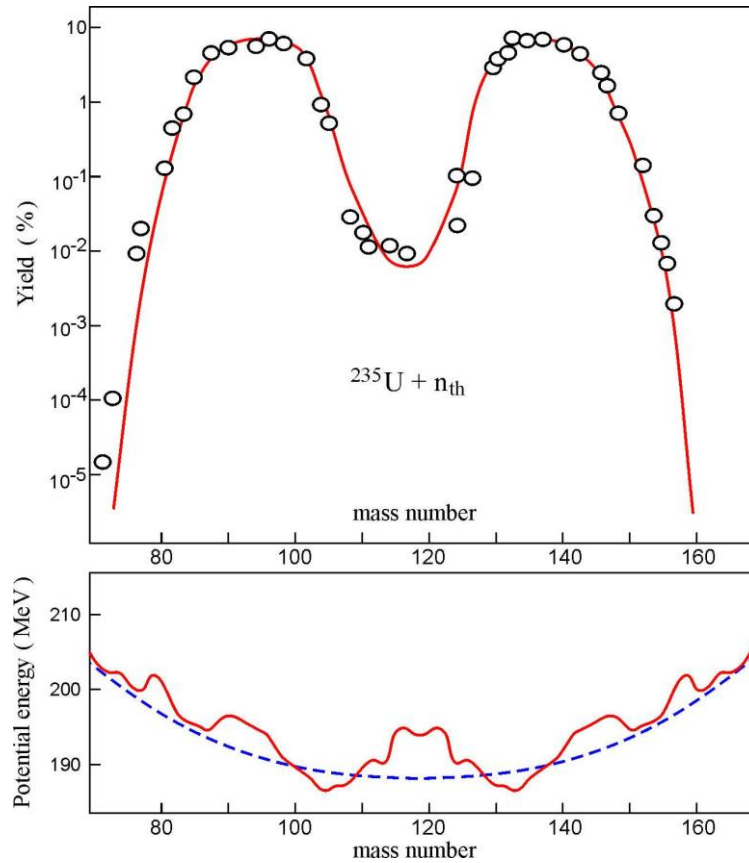


Fig. 1.4 Upper panel (taken from [6]): mass distribution of fragments for thermal-neutron-induced fission of ^{235}U (relative yield). The theoretical curve corresponds to the calculation by the empirical Fong formula [7]. The lower panel shows the potential energy of two fission fragments at the distance 16 fm from each other calculated within the liquid-drop model [1] (dashed curve) and the two-center shell model [8] (solid curve).

Strong asymmetry in the yield of the fission fragments indicates that at low excitation energy structural effects, namely, the shell effects in the fissioning nucleus and in the forming fission fragments play a significant role in the dynamics of fission. The lower panel of Fig. 1.4 shows the potential energy of interaction between the two fission fragments (whose centers are at the distance 16 fm from each other) depending on the mass distribution between them. It is known that any physical system tends to the minimum of the potential energy in its evolution. In case of the liquid-drop model the potential energy minimum corresponds to symmetric fission, which contradicts the experiment. Taking into account quantum effects (shell structure of the nucleus fissioning during its deformation and transition to the two fission fragments) within the two-center shell model [8] leads to the minimum of the potential energy for the formation of fragments with masses around 102 and 134. This is due to the increased stability (higher specific binding energy) of nuclei with masses 132-140 having the closed neutron shell $N = 82$ and the number of protons close to the magic number $Z = 50$.

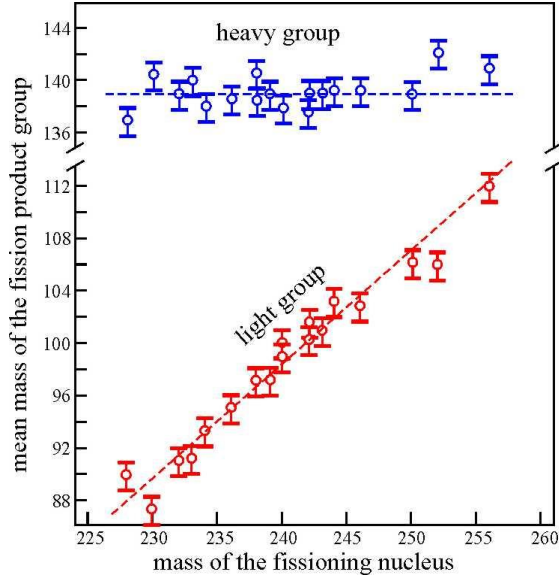


Fig. 1.5 The average value of the mass of light and heavy fission fragment groups depending on the mass of the fissioning nucleus (figure was taken from [4]). Dashed lines are drawn for clarity.

It is these nuclei that are formed as heavy fragments in the fission of all weakly excited transuranium elements (see Fig. 1.5). The mass of light fragments increases linearly with the mass of the fissioning nucleus as they simply complement the mass of the strongly bound heavy fragments $A_{light} = A - A_{heavy} (\approx 140)$. It is clear that if we increase the mass of the nucleus up to the value $A \sim 280$ mainly symmetric fission must be observed, and when $A > 280$ it is a light fragment that will have the mass about 140, whereas the mass of the heavy fragment must increase linearly with increasing A (i.e. the dashed curves in Fig. 1.5 must simply cross). Precisely this is what is observed in the fission of superheavy nuclei.

Of course as already mentioned the process of fission of the nucleus occurs in the multidimensional parameter space (its elongation, deformation of nascent fragments, mass and charge asymmetry). However, even simple “energy” estimates made within the statistical model and taking into account the higher level density in the fragments formed in the channels with large energy release give a qualitatively correct description of the mass distribution. In one of these models (Fong model [7]) the probability of formation of the fragments (Z_1, A_1) and (Z_2, A_2) is given by the simple formula

$$Y_f(Z_1, A_1, Z_2, A_2) \sim \int_0^{Q_f} dE_{kin} \int_0^{Q_f - E_{kin}} \rho_1(\varepsilon_1) \rho_2(\varepsilon_2 = Q_f - E_{kin} - \varepsilon_1) \mu^2 E_{kin} d\varepsilon_1,$$

where the numbers 1 and 2 denote two fission fragments, $\varepsilon_{1,2}$ is their excitation energy, E_{kin} is the kinetic energy of the fragments, and $Q_f = M(Z, A)c^2 - M(Z_1, A_1)c^2 - M(Z_2, A_2)c^2$ is the total energy released during fission of the nucleus (it just depends on Z_1, A_1 and Z_2, A_2), $Q_f = E_{kin} + \varepsilon_1 + \varepsilon_2$. Level densities ρ_1 and ρ_2 of nuclei (Z_1, A_1) and (Z_2, A_2) with excitation energies ε_1 and ε_2 , respectively, play a key role in this formula. Since the level density of nuclei is exponentially dependent on their excitation energy $\rho(\varepsilon) \sim \exp[2\sqrt{a\varepsilon}]$, the yield of fragments will be maximum in those channels where the energy release Q_f is larger. The theoretical curve in the upper panel of Fig. 1.4 was obtained in [6] just within the Fong model. Thus, this model satisfactorily describes the mass distribution of the fragments.

1.4 Kinetic energy of fission fragments

Most part of the total energy released during fission is removed in the form of the kinetic energy of the fission fragments and the rest - in the form of the excitation energy of the fragments $Q_f = E_{kin} + \varepsilon_1 + \varepsilon_2$. If we assume that at the time of scission of the fissioning nucleus fragments have a zero initial velocity (i.e. nuclear liquid is quite viscous), then at a great distance their kinetic energy will be determined by their potential energy at the point of scission. If the scission occurs at the distance R between the centers of the fragments, then (neglecting deformations) their potential energy of interaction is close to the Coulomb repulsion energy of the fragments $V_{Coul} = \frac{Z_1 Z_2 e^2}{R}$ which eventually transforms into the kinetic energy at large distances. Assuming $Z_1 = Z_2 = Z/2$, $R \sim R_1 + R_2 = r_0 A_1^{1/3} + r_0 A_2^{1/3} = const \cdot A^{1/3}$, we conclude that the kinetic energy of the fission fragments must be proportional to the factor $Z^2 / A^{1/3}$, where Z and A are the charge and the mass of the fissioning nucleus. Precisely this is what is observed in the experiment, see Fig. 1.6.

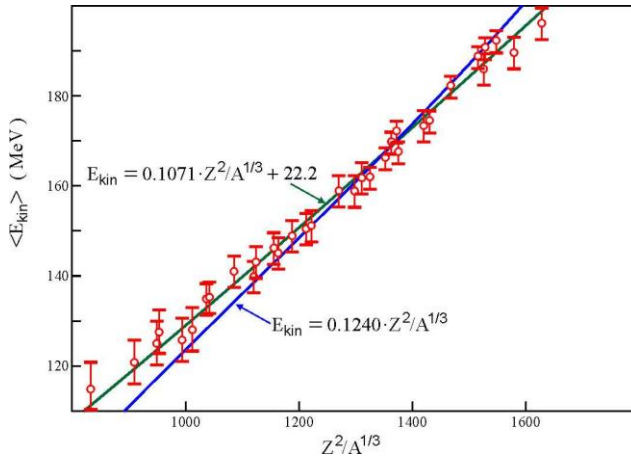


Fig. 1.6 Dependence of the most probable kinetic energy of fission fragments on the Coulomb energy parameter $Z^2 / A^{1/3}$ (Z and A are the charge and the mass of the fissioning nucleus). Figure was taken from [4]. The curves in the figure and the corresponding formulas are called the Viola systematics [9].

The described above simplified scenario of fission, slow (due to the strong nuclear viscosity) descent from the height of the nuclear fission barrier to the scission point is also confirmed by the fact that the kinetic energy of the fission fragments is weakly dependent on the excitation energy of the fissioning nucleus (which just transforms into the additional excitation energy of fragments).

References

- [1] W. D. Myers and W. J. Swiatecki, Ark. Phys. **36**, 343 (1967).
- [2] V. M. Strutinsky, Nucl. Phys. **A95**, 420 (1967).
- [3] P. Möller, J. R. Nix, W. D. Myers, and W. J. Swiatecki, At.Data **59**, 185 (1995).
- [4] R. Vandenbosch and J. R. Huizenga, *Nuclear Fission*, Academic Press, New York, 1973.
- [5] <http://nrv.jinr.ru/nrv/webnrv/fission/>.
- [6] L. Willets, *Theories of nuclear fission*, Clarendon Press, Oxford 1964/
- [7] P. Fong, Phys. Rev. **102**, 434 (1956).
- [8] J. Maruhn, W. Greiner, Z. Phys. A **251**, 431 (1972).
- [9] V.E. Viola, Jr., Nucl. Data Tables **A1**, 391 (1966).

2. Time-of-flight method for measuring mass-energy distributions of products of binary nuclear reactions

2.1 Time-of-flight methods

To measure the binary products of nuclear reactions several different approaches are used: a) measuring the energies of the two fragments (2E method); b) measuring the velocities of the two fragments (2V method); c) measuring the speed and energy of one fragment (V-E method); d) measuring the speed and energy of the two fragments (2V-2E method). The latter method provides the most complete information about the binary reaction products.

In the 2V method the velocities measured in the experiment and the derived from them values of mass and energy correspond to the primary fragments; as neutron emission is isotropic in the rest system of the fission fragment the values of the average velocity of each of the fragments do not change after evaporation of neutrons. In case of the 2V experiments the spread of velocity due to the neutron emission leading to inaccuracies in the calculated masses of the fragments is less than in the 2E experiments. Thus, obtaining a good time resolution becomes the main requirement for the experimental setup to obtain a good mass and energy resolution.

2.2 2V time-of-flight method

Fission of the formed in the reaction heavy nucleus with the mass M_{tot} moving with the velocity \vec{v} is accompanied by the emission of two lighter nuclei (fission fragments) with masses m_1 and m_2 and velocities \vec{v}_1 and \vec{v}_2 , respectively (Figure 2.1.). By the law of momentum conservation $m_1 \vec{v}_1 + m_2 \vec{v}_2 = M_{tot} \vec{v}$. In the experiment, as a rule, it is required to determine the characteristics (energy, charge and mass) of produced fragments of the reaction. The time-of-flight method just allows you to measure the velocities and masses of these fragments.

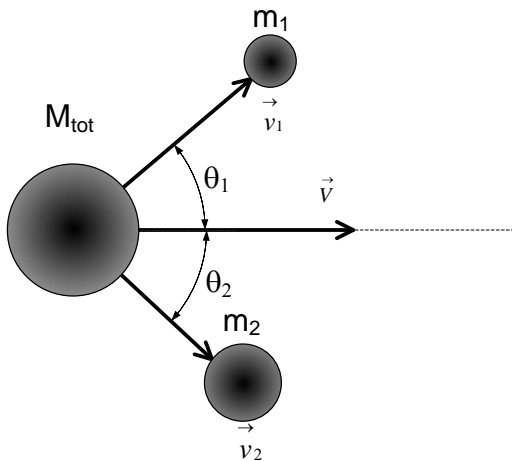


Fig. 2.1 Fission of the nucleus with the mass M_{tot} and the velocity \vec{v} .

In case of spontaneous fission or fission by slow neutrons (when the fissioning nucleus is at rest and $\vec{v} = 0$) the situation is somewhat simplified, but does not fundamentally change. The sample containing spontaneously fissioning nuclei with the known mass M_{tot} is in the center of the experimental setup (see next section). After the decay the emitted fragments formed in the fission process are detected by the opposite arms of a spectrometer. Each arm of the spectrometer consists of the start and stop detectors and has the path length l . The stop detectors are position sensitive i.e. it is known what part of the detector the particle hit.

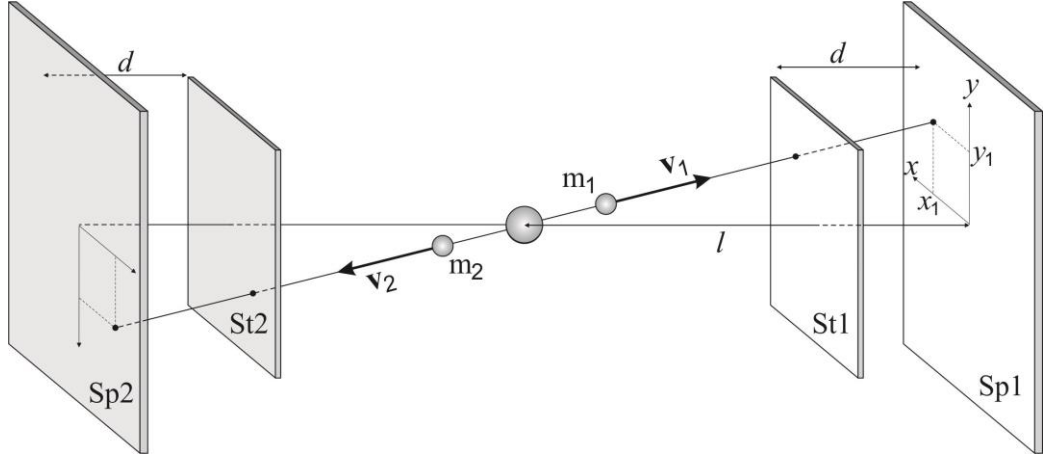


Fig. 2.2 Schematic representation of the time-of-flight spectrometer.

If fission fragments hit the arms of the spectrometer the time of the hit is registered by the start detector (t_{St1} , t_{St2}). Also using the stop detectors the time and the hit coordinates in each of the detectors (t_{Sp1} , x_1 , y_1 , t_{Sp2} , x_2 , y_2) are registered. Calculating for the fragment the time difference between entering and leaving the arm of the spectrometer we determine the time of flight of the path length d :

$$t_{tof1} = t_{Sp1} - t_{St1} \quad (2.1)$$

$$t_{tof2} = t_{Sp2} - t_{St2} \quad (2.2)$$

Then it is necessary to calculate the emission angles of fragments in and out of the reaction plane (Θ_1 , Θ_2 , ϕ_1 , ϕ_2). The angles are calculated as follows:

$$\Theta_{x1} = \arccos \frac{l}{\sqrt{l^2 + x_1^2}} \quad (2.3)$$

$$\Theta_{y1} = \arccos \frac{l}{\sqrt{l^2 + y_1^2}} \quad (2.4)$$

$$\Theta_{x2} = \arccos \frac{l}{\sqrt{l^2 + x_2^2}} \quad (2.5)$$

$$\Theta_{y2} = \arccos \frac{l}{\sqrt{l^2 + y_2^2}}, \quad (2.6)$$

where x_1 , x_2 , y_1 , y_2 are the coordinates of the particles in the first and the second detector respectively, and l is the distance to the center of the stop detector. The emission angle of fission fragments in the laboratory system will be equal to:

$$\Theta_{1,2} = \arccos \{ \cos \Theta_{1,2} \cos \phi_{1,2} \} \quad (2.7)$$

As the path length d is known it is now possible to calculate the velocity of each of the fragments:

$$v_1 \cos \Theta_1 = \frac{d}{t_{tof1}} \quad (2.8)$$

$$v_2 \cos \Theta_2 = \frac{d}{t_{tof2}} \quad (2.9)$$

The masses of fission fragments are calculated using the assumption of a two-body process and the law of total momentum conservation:

$$M_{tot} = m_1 + m_2 \quad (2.10)$$

$$M_{tot} \vec{v} = m_1 \vec{v}_1 + m_2 \vec{v}_2 \quad (2.11)$$

Taking into account that the velocity of the initial nucleus is equal to zero ($v=0$) and the momenta of the fragments are in the opposite directions from the expressions (2.10) and (2.11) we obtain:

$$m_1 = \frac{M_{tot} v_2 \sin \Theta_2}{v_1 \sin \Theta_1 + v_2 \sin \Theta_2} \quad (2.12)$$

$$m_2 = M_{tot} - m_1 \quad (2.13)$$

It is important to note that in determining the initial velocity of the fragments we must consider their energy loss in the foils of the start detectors (loss in the foils and the emission angle corrections are taken into account in the data processing program). The value of the total kinetic energy released in fission was determined from the relationship:

$$E_k = \frac{1}{2} (m_1 v_1'^2 + m_2 v_2'^2). \quad (2.14)$$

where v_1' and v_2' are the velocities of the fragments in the center of mass system.

3. Description of experimental setup

3.1 General outline of setup

- Stand spectrometer consists of the reaction chamber (1) where the target assembly (3) is located and the two identical time-of-flight position-sensitive arms (2). Each arm includes start and stop detectors based on MCP;
- vacuum pumping system (6);
- system converting analog signals to digital signals (7);
- data acquisition system (7);
- software.

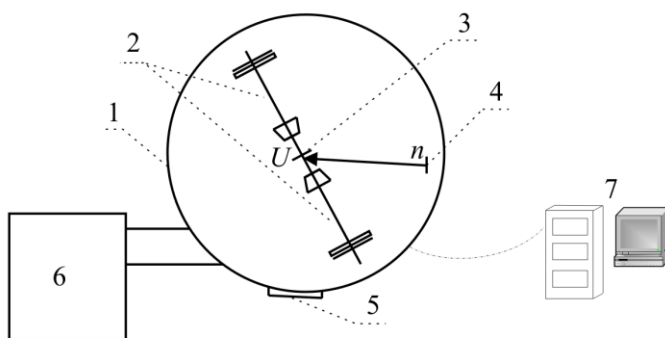


Fig. 3.1. Schematic representation of the stand spectrometer and a general view of the setup.

3.2 Reaction chamber

The reaction chamber is designed for mounting of the detectors based on microchannel plates as well as the target assembly. The design of the camera allows you to obtain the 10^{-6} Torr vacuum. The target assembly where radioactive targets are mounted is located in the center of the chamber.



Fig. 3.2. Photo of the reaction chamber and detectors.

3.3 Start detector

The principle of operation of the start detector is based on the use of secondary emission of electrons knocked out by a particle from the conversion foil of the detector. The scheme of the detector is presented in Fig. 3.3. The detector consists of the conversion foil (the input window in Fig. 2), an accelerating grid, an electrostatic mirror, a chevron assembly of microchannel plates (MCP),

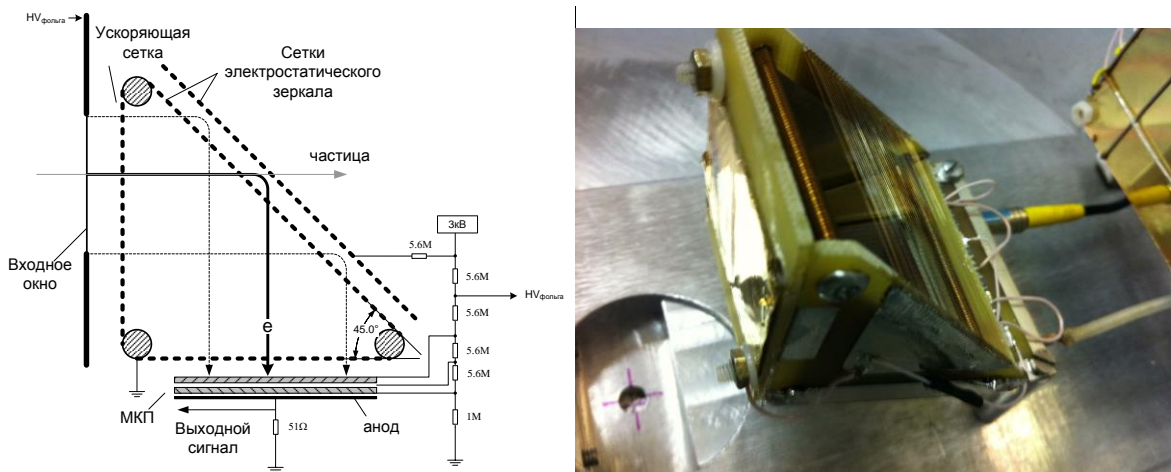


Fig. 3.3. Scheme of the start detector and photo of the detector.

The time resolution of the start detector is determined by the time-of-flight spectrum of alpha particles from ^{226}Ra measured by two identical start detectors with different path lengths and will be ~ 150 ps. When registering heavier ions the resolution of the start detector will be ~ 120 ps. Transparency of the start detector is approximately 82 %.

3.4 Stop detector

The stop detector scheme is shown in Fig. 3.4. It consists of a conversion input foil, a chevron assembly of two MCP plates, a coordinate system as well as a PCB with fast preamplifiers of time and coordinate signals.

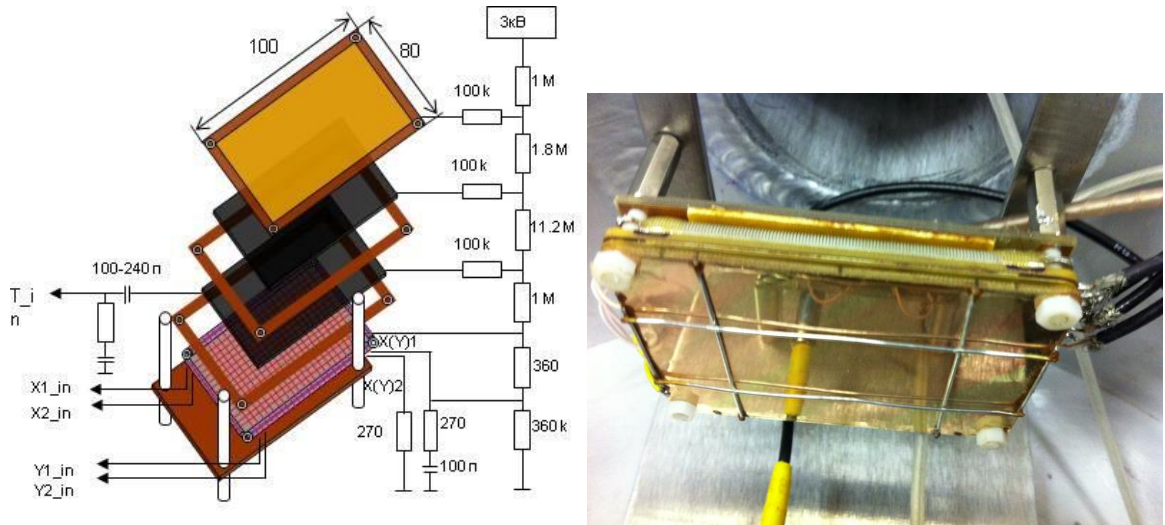


Fig. 3.4. Scheme of the stop detector and photo of the stop detector.

3.5 Vacuum system

The vacuum pumping system is designed to provide necessary vacuum for the normal operation of the detectors. The pumping system consists of a backing pump for preliminary pumping, turbo-molecular pump to obtain high vacuum (providing pumping up to 10^{-7} Torr vacuum) as well as an oil trap, vacuum valves and bellows. The backing pump provides pumping up to 10^{-2} Torr vacuum, which creates the necessary conditions to switch on the turbo-molecular pump. The turbo-molecular pump provides pumping up to 10^{-7} Torr vacuum, which creates conditions for the measurement.



Fig. 3.6. Photo of the pumping system.

3.5 Data acquisition system

The data acquisition system consists of the CAMAC standard electronic blocks and a computer. A time-to-digital converter (TDC) is the key device registering the time during which a particle passes the spectrometer arm. (For more details, see Appendix 1).

The computer data acquisition system KMAX is used in the measurements. This system allows accumulation, processing and recording of hundreds of parameters of the event on the disk of the personal computer (in case of measuring not only fission fragments, but also the accompanying emission of light particles and gamma rays).

3.6 Main characteristics of setup

Table 1 summarizes the main characteristics of the setup. Values are given for the 10 cm path length between the target and the stop detector, the size of the stop detector is 43 x 63 mm.

Time resolution of each arm	150 ps
Angular resolution - in the reaction plane - out of the reaction plane	$\approx 0.5^\circ$ $\approx 0.5^\circ$
Geometric efficiency of spectrometer	$\approx 3\%$
Detection efficiency	$\sim 50\%$
Mass resolution of spectrometer (FWHM)	3 amu

Time resolution of each arm is defined as the minimum time that must separate two events (the arrival of particles in the arm of spectrometer) to be registered as two separate events.

Angular resolution is the accuracy of determining the angle at which the particle left the source.

Geometric efficiency of spectrometer is the ratio of the number of registered particles to the total number of particles emitted by the source.

Detection efficiency is the probability that the particle that hit the arm of the spectrometer will be registered.

Mass resolution of spectrometer is the accuracy of determining the mass of detected particles. (Conventionally the resolution of the detector in absolute units is the full width at half maximum (FWHM)).

4. Instructions on performing measurements of mass-energy distributions of fission fragments using time-of-flight method on “ToF” setup

4.1 General principles

The “ToF” setup is designed to measure mass-energy distributions of fission fragments on the basis of the time-of-flight method. The setup consists of the following components: (1) vacuum chamber, (2) vacuum pumping system, (3) stand with electronics, computer. Ra and Cm radioactive sources of low intensity, high-voltage power supplies with voltage above 1000 V, electric power supply with voltage 220 V are used on the “ToF” setup.

When working on the setup you should follow these instructions, terms of personnel arrangements on the work in the fields of ionizing radiation at JINR, the instruction No. 42-362P “On fire safety” and joint actions of personnel and fire department on fire suppression at “ToF” setup for measuring mass-energy distributions of fission fragments on the basis of the time-of-flight method in room 222, building 131, FLNR JINR, instructions I1-I3.

The power supply of electric circuits of the setup is provided by the electric service panel IIIП-2 Гр-2 with the voltage 220/380 V.

4.2 Pumping of reaction chamber

Power on computer, crate, vacuum system from the 220 V outlet

Using the VM1 vacuum device make sure that the pressure in the reaction chamber corresponds to the atmospheric pressure (~760 Torr). If the pressure in the chamber is different from the atmospheric pressure, then let in air into the chamber by gradually opening the valve N1. After the pressure in the chamber reaches the atmospheric pressure, close the valve N1. If the pressure in the reaction chamber corresponds to the atmospheric pressure, then proceed to the pumping of the chamber.

- a) make sure that the valve V1 on the backing pump is closed,
- b) open the valve V2 on the camera,
- c) by toggle switch on the backing pump,
- d) open the pumping valve V3 of the turbo-molecular pump,
- e) gradually open the valve V1 until the pressure inside the chamber reaches 2×10^{-2} Torr (follow the indications on the vacuum device VM1).

Switch on the turbo-molecular pump using the control unit БУ-150.

To do this:

- a) press the “Сеть” button on the unit БУ-150
- b) press the “26000” button
- c) close the valve V2.
- d) when the indicator “f норм” is on, press the “42000” button
- e) wait until the indicator “f норм” is on again.

Wait until the pressure inside the reaction chamber reaches the value 3×10^{-5} Torr. (follow the indications on the vacuum device VM1).

4.3 Switching on detectors.

Supply high voltage to the detection part of the setup. Gradually increase the high voltage on the blocks HVST1, HVST2, HVSP1, HVSP2.

Switch on preamplifiers +6 V and +24 V (to do this it is necessary to connect the cables “+6V” and “+24V” to the corresponding connectors on the crate).

Before performing the following step, it is necessary that you familiarize yourself with the principle of operation of an oscilloscope!

Check availability and the amplitude of signals from preamplifiers on the oscilloscopes St1, St2, Sp1, Sp2, X1, X2, Y1, Y2. (To do this, disconnect the cable “St1” from the module “C.F.D.” and connect it to the connector of the oscilloscope. After checking availability of the signal, return the cable to the previous connector in the crate. Perform this operation in sequence for cables “St1”, “St2”, “Sp1”, “Sp2”, “X1”, “X2”, “Y1”, “Y2”).

4.4 Performing data acquisition for later processing

During operation, monitor the proper functioning of the setup components.

Upon detection of malfunctioning that may cause an emergency situation and lead to an accident, completely switch off power on the setup and take measures to prevent the emergency situation.

Switch on the computer. (Warning: for correct work of the system the computer can only be switched on when the crate is on).

Start the Kmax program by double-clicking on the “Kmax-8” icon

Open the file necessary for data acquisition “Stend.tlsh” (File→Open Toolsheet→Stend.tlsh)

On the “Control Panel” tab clear all the histograms by clicking the button “Clear Histograms”.

Open a new data file specifying an arbitrary name (File→New Event File).

Start data acquisition by clicking the “Start” button.

On the tab “Tof-Tof Histograms” make sure that the data acquisition is in progress (histograms are being filled).

After acquiring sufficient statistics stop data acquisition by clicking the “Stop” button on the “Control Panel” tab.

Close the data file (File→Close Event File).

Close the Kmax program.

4.5 Filling reaction chamber and switching off detectors

Switch off high voltage on the detectors HVST1, HVST2, HVSP1, HVSP2.

Switch off the turbo-molecular pump using BY-150 (to do this it is necessary to press the “сеть” button).

Shut off the valve V1 on the backing pump.

Switch off the backing pump and wait for 30 minutes until the full stop of the turbo-molecular pump.

Gradually fill the reaction chamber with air through the valve N1.

Open the camera.

After work

Switch off the electronics and the computer.
Inspect the setup.
Make the necessary journal notes.

Fire safety measures

Employees authorized to work at the “ToF” setup, room 222, building 131, FLNR must carry out the work in accordance with the instruction No. 42-362P “On fire safety and joint actions of personnel and fire department on fire suppression at “ToF” setup”.

Radiation safety measures

Work at the setup is carried out in accordance with the instruction No. 42-263R on radiation safety when conducting experiments in room 214, building 101, FLNR, JINR and the instruction No. 42-106R.

Safety requirements in case of emergency

In case of fire detection or signs of burning in the room of the “ToF” setup (smoke, smell of burning, rise of temperature, etc.), act in accordance with the instruction No. 42-362P “On fire safety and joint actions of personnel and fire department on fire suppression at “ToF” setup”. In case of emergency radiation situation, act in accordance with the instruction 42-106R.